CellPress

Cell
Leading Edge

Primer

The epitranscriptome toolbox

Sharon Moshitch-Moshkovitz,[1,2,3] Dan Dominissini,[1,2,3] and Gideon Rechavi[1,2,3,*]
[1]Cancer Research Center, Sheba Medical Center, Tel Hashomer, Israel
[2]Sackler School of Medicine, Tel Aviv University, Tel Aviv, Israel
[3]Wohl Institute for Translational Medicine, Sheba Medical Center, Tel Hashomer, Israel
*Correspondence: gidi.rechavi@sheba.health.gov.il
https://doi.org/10.1016/j.cell.2022.02.007

SUMMARY

In the last decade, the notion that mRNA modifications are involved in regulation of gene expression was demonstrated in thousands of studies. To date, new technologies and methods allow accurate identification, transcriptome-wide mapping, and functional characterization of a growing number of RNA modifications, providing important insights into the biology of these marks. Most of the methods and approaches were developed for studying m^{6}A, the most prevalent internal mRNA modification. However, unique properties of other RNA modifications stimulated the development of additional approaches. In this technical primer, we will discuss the available tools and approaches for detecting and studying different RNA modifications.

INTRODUCTION

Chemical modifications of RNA were identified in highly abundant non-coding RNA species such as ribosomal and transfer RNAs (rRNA and tRNA, respectively) more than half a century ago (reviewed in Stacey, 1965). These RNA species consist of over 160 modified nucleotides (Boccaletto et al., 2018). In the last decade, a growing number of modifications was also identified and characterized in low abundance species of RNA, namely mRNA and long non-coding RNA (lncRNA). The collection of these modifications, termed the epitranscriptome, includes N^6-methyladenosine (m^{6}A) (Dominissini et al., 2012; Meyer et al., 2012), N^1-methyladenosine (m^{1}A) (Dominissini et al., 2016; Li et al., 2016), inosine (Levanon et al., 2004), 5-methylcytidine (m^{5}C) (Squires et al., 2012), 5-hydroxymethylcytidine (Delatte et al., 2016), pseudouridine (Carlile et al., 2015; Li et al., 2015; Schwartz et al., 2014), N^6,2'-*O*-dimethyladenosine (Mauer et al., 2017; Akichika et al., 2019; Sun et al., 2019), N^4-acetylcytidine (Arango et al., 2018), N^7-methylguanosine (m^{7}G) (Zhang et al., 2019), and 2'-*O*-methylated nucleotides (Nm) (Dai et al., 2017). mRNA modifications embed transcripts with additional information over their canonical sequence to finely regulate gene expression through altering charge, base-pairing potential, RNA folding, and RNA-protein interactions.

The vast majority of the information regarding the field of epitranscriptomics was acquired from studying m^{6}A, the most prevalent, internal (non-cap) mRNA modification. Hundreds of studies uncovered the machineries that install (writers), remove (erasers), and bind (readers) m^{6}A to exert its functions. These studies exposed a novel regulatory layer of gene expression that affects almost every step in mRNA metabolism from transcription to decay (Zaccara et al., 2019). As data on m^{6}A accumulated rapidly, other mRNA modifications were identified, igniting the search for their writers. However, unlike m^{6}A, which is installed in mRNA by a dedicated writer complex (Zaccara et al., 2019), distinct from the machineries that install it in rRNA (van Tran et al., 2019; Ma et al., 2019), other mRNA modifications appear to be installed by the same writers that act on rRNA, tRNA, and other abundant non-coding RNAs. This pronounced redundancy of substrate RNA species poses an obstacle for experimentally targeting mRNA modifications without affecting other essential machineries (tRNA/rRNA/small nuclear RNA [snRNA]) (Schaefer, 2021; Esteve-Puig et al., 2020). Thus, while studies draw a clear and detailed picture of the roles of m^{6}A in gene expression regulation, there are substantial knowledge gaps regarding the roles and mechanisms of most of the other mRNA modifications.

Detection of new epitranscriptomic marks emphasized the need for improved mapping methods and stimulated the development of a wide range of tools. These tools combine new profiling strategies including enrichment approaches, identification of reverse transcription signatures, or manipulation of the unique properties of the modification, enabling its study and characterization in lower-abundance RNA species.

Here, we discuss different tools and approaches for studying RNA modifications, and revealing their functions. The exponential growth of epitranscriptome research led to the development of multiple methodologies, and their detailing is beyond the scope of this primer. We discuss below the basic approaches that should be taken when studying a new epitranscriptomic mark (Figure 1).

DETECTION

Multiple RNA modifications (Boccaletto et al., 2018) expand the nucleotide repertoire of RNA. In order to study a given (known) modification either in a specific subset of RNA molecules or in the transcriptome of an organism, where it was already identified, the first step is to detect it and estimate its abundance.

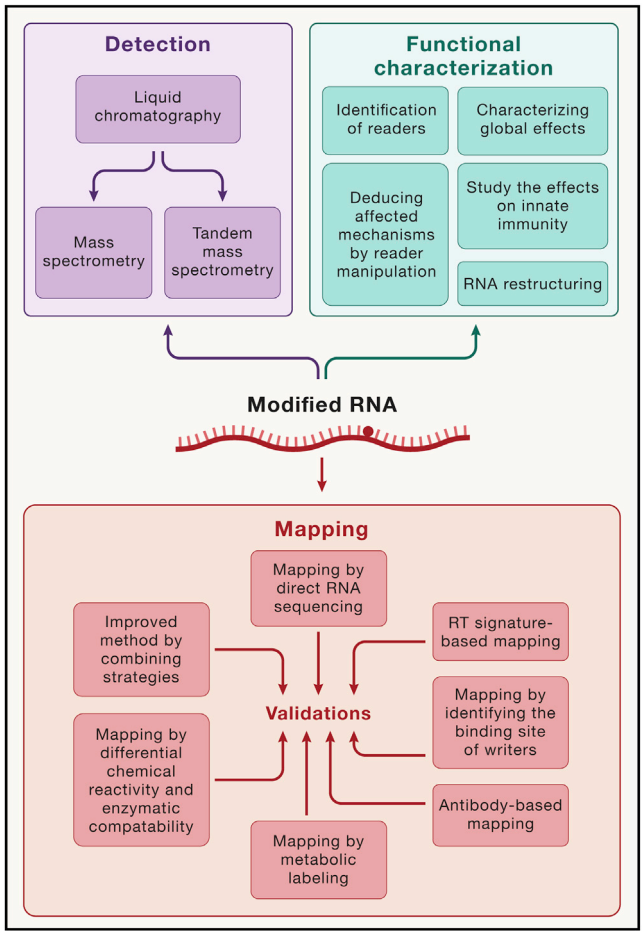

Figure 1. The technical approaches described in the paper for detection (purple), mapping (red), and functional characterization (green) of different RNA modifications

Many next-generation sequencing (NGS)-based methods (discussed below) map RNA modifications in a transcriptome-wide manner, revealing their profiles in normal and pathological states in different cells, tissues, and organisms and under different environmental conditions and stimuli. While mapping tools produce gene-specific profiles, they are often blind to quantitative data, stoichiometry, and dynamics. In past decades, traditional approaches for quantifying individual RNA modifications were based mainly on semiquantitative methods such as two-dimensional thin-layer chromatography (TLC) (Keith, 1995) and liquid chromatography (LC) (Desrosiers et al., 1974) that analyze nucleotides or nucleosides by comparison to known standards. Such methods are unsuitable for analyzing many modifications concomitantly, are labor- and time-consuming, and often involve radioactive labeling. The rapid development of the epitranscriptomics field raised the need for high-throughput, accurate, and sensitive detection methods to bridge the gap between epitranscriptomic profiles and quantification of dynamic changes in modification levels.

Mass spectrometry (MS) has been extensively used in proteomics and metabolomics to identify and quantify individual molecules in a mixture. Adopting this approach enables analysis of a mixture of RNA nucleosides by MS to simultaneously identify and quantify multiple modifications in a sample. The most common quantitative MS approach for assessment of RNA modifications is performed on single nucleosides using LC coupled to MS (LC-MS) or tandem MS (LC-MS/MS). The RNA sample is enzymatically digested and dephosphorylated into single nucleosides that are separated by LC and analyzed by MS (Su et al., 2014). Identification of the different nucleosides in the mixture is based on their biophysical properties including molecular mass, chromatographic retention time, and fragmentation pattern (Su et al., 2014). The triple validation of the nucleoside's identity according to the above three biophysical properties confers this method its high accuracy. However, this method excludes the 5′ cap-associated nucleotides of mRNA transcripts from the analysis, as the commonly used non-specific nucleases (such as P1) fail to break the bond between m^7G of the 5′ cap and the first transcribed nucleotide, releasing mononucleotides and cap-dinucleotides. This limitation can be overcome, and cap-associated modified nucleotides can be quantitatively identified by LC-MS/MS analysis based on comparison to known cap-dinucleotide standards, rather than single nucleosides (Wang et al., 2019; Galloway et al., 2020).

Various MS instruments differ in their precision. Simple instruments, such as a single-quadrupole MS, include a low-resolution MS, lacking the ability to fragment. Such instruments depend on chromatography for separating all isobaric species and can identify modified nucleosides at the monoisotopic mass level (Lauman and Garcia, 2020). High-resolution instruments, such as the triple-quadrupole MS, can perform tandem MS (MS/MS) and are capable of fragmentation. These instruments can, therefore, accurately differentiate and identify nucleosides of identical mass (Su et al., 2014). In addition, due to the high sensitivity, LC-MS/MS enables detection and quantification in the femtomole to attomole range (Basanta-Sanchez et al., 2016; Sarin et al., 2018). Protocols that incorporate metabolically labeled nucleosides further increase detection specificity and accuracy and improve comparative analyses (Wetzel and Limbach, 2016). Nucleoside labeling uses stable isotopes such as ^{18}O (Li and Limbach, 2012), $^{13}C/^{15}N$ (Paulines and Limbach, 2017), or ^{3}H (Dominissini et al., 2016).

In principle, LC-MS/MS can also be used to map RNA modifications in RNA fragments to provide a site-specific context (Solivio et al., 2018). However, this method requires fine adjustment of the fragmentation step to ensure transcript breakdown into short overlapping fragments and hundreds of nanograms of each transcript, making it unsuitable for analysis of mRNAs, due to the relatively low abundance of individual transcripts and the large diversity in the transcriptome (Solivio et al., 2018).

The use of LC-MS/MS offers quantitative analysis of multiple RNA modifications in one sample at high precision. The main advantage of this method is in its high specificity and sensitivity. Unlike sequencing-based mapping tools, MS has a very low false detection rate due to the triple parameter-based identification of nucleosides (retention time, mass, and fragmentation pattern), and it is highly reproducible. However, the main limitation of MS analysis is that it can only analyze modifications that are specified *a priori* (Su et al., 2014; Basanta-Sanchez et al.,

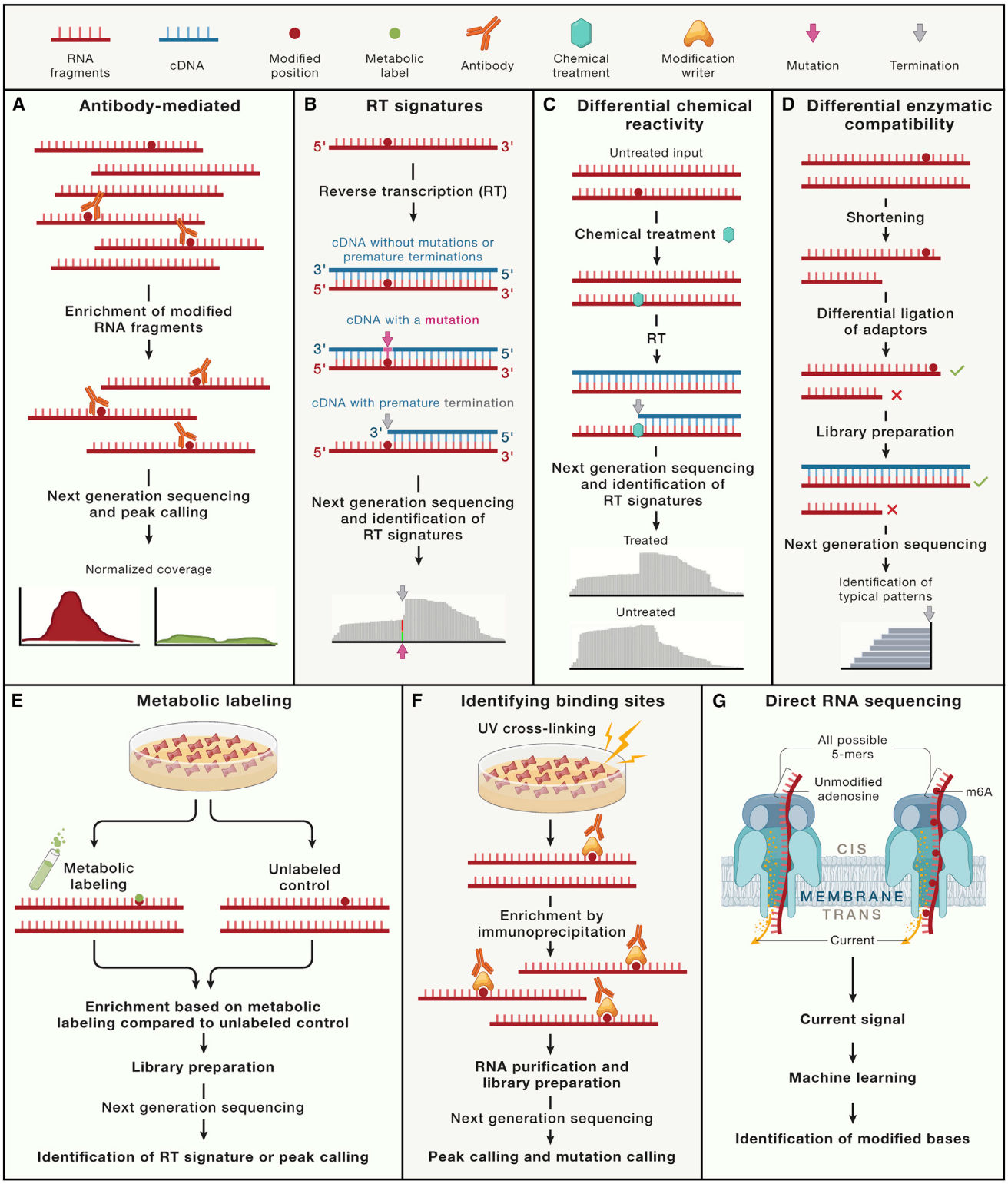

Figure 2. A schematic illustration of the main mapping strategies for RNA modifications

(A) Antibody-mediated mapping.

(B) Mapping by RT signatures.

(C) Mapping by differential chemical reactivity.

(legend continued on next page)

2016), meaning that novel or unidentified nucleosides are disregarded from the analysis. Another drawback is that since transcripts are digested into single nucleosides during sample preparation, the identity of the modified transcript is lost. Moreover, the high sensitivity of MS serves as a double-edged sword when analyzing mRNA. Since MS can detect quantities in the attomolar range, any residual contamination or degradation of rRNA or tRNA (that are highly enriched in modifications) in the sample may result in false estimation of rare mRNA modifications.

MAPPING

Quantitative assessment of a given RNA modification is only the first step in the process of its characterization. The next imperative step is to map its positions at the transcriptomic level, with respect to other transcript attributes. Mapping RNA modifications can be divided into several approaches: (1) modifications that alter Watson-Crick base-pairing or interfere with the reverse transcription (RT) process. These modifications leave a typical mark in the cDNA called RT signatures. (2) Modifications that exhibit differential compatibility with certain enzymatic reactions or differential chemical reactivity with specific reagents. (3) Different mapping tools combine several approaches to obtain more effective, accurate, and selective profiling. The large number of available methods reflects the lack of perfect methods and explains why imperfect methods, each with its disadvantages and benefits, are still being pursued in the field.

An important part of mapping is the bioinformatic analysis that identifies modified sites based on the sequencing results. This analysis takes into account statistical and computational parameters, based on the experimental approach and controls, in order to minimize false-positive site calling. As the data in the field accumulated, enigmatic and sometimes opposite findings have surfaced, some of which were attributed to differences in the computational approach taken.

For example, two m^1A studies that took a similar experimental approach reached very different conclusions. These major differences can be attributed, at least in part, to major differences in the analysis criteria and pipelines including coverage thresholds, read collapse, and misincorporation analysis (Dominissini and Rechavi, 2017). Establishing reliable bioinformatics pipelines improves site identification and reduces inconsistencies.

Antibody-based mapping

Efficient mRNA mapping protocols often consist of enrichment steps, using highly specific antibodies, to increase the relative abundance of the modification of interest prior to sequencing. Antibody-mediated capture of RNA fragments, coupled to NGS (Figure 2A), requires high amounts of starting material and does not provide single-base resolution (the resolution depends on fragment size). Moreover, the level of noise, especially when analyzing low-abundance modifications, may lead to higher false detection rates, resulting from non-specific binding of RNA fragments to the beads used for enrichment. False site detection may also result from cross-reactivity of the antibody with other modifications. Several measures should be taken to avoid false detection.

Antibody specificity should be determined either by dot blot with suspected cross-reactive modifications (Linder et al., 2015), or by quantitative MS analysis of the nucleoside composition in RNA fragments enriched by the antibody, to detect any other co-enriched contaminating modifications. Additional means to reduce noise include bead-only controls, competitive elution (Dominissini et al., 2013), or comparison to an unmodified matching RNA sample (after genetic, chemical, or enzymatic removal of the modification; (Geula et al., 2015; Dominissini et al., 2016; Li et al., 2017; Zhang et al., 2021). Another limitation of this approach is that it is blind to modification stoichiometry as well as to splice variants.

Antibody-based mapping of m^6A generated transcriptome-scale maps consisting of thousands of sites in human and mouse and exposed its non-random distribution and a conserved sequence motif of RRACH (R = A or G, and H = A, C or U) (Dominissini et al., 2012; Meyer et al., 2012). Superimposing m^6A positions on other transcript attributes uncovered the first biological roles of m^6A in regulation of transcript stability and splicing (Dominissini et al., 2012; Meyer et al., 2012). The uncovering of the first m^6A methylomes jump-started a large number of studies and marked the beginning of the era of epitranscriptomics. However, anti-m^6A antibodies bind both m^6A and m^6Am, both of which contain a methyl group on the N^6 position of adenosine. Thus, transcriptome-wide mapping of m^6A also includes mis-annotated m^6Am sites (Linder et al., 2015). Due to the significantly greater mRNA prevalence of m^6A over m^6Am (ranging from 10- to 15-folds), this cross reactivity poses a greater problem when mapping m^6Am. m^6Am sequencingeq maps and differentiates m^6Am from 5′-UTR m^6A sites and combines enrichment of 5′cap-containing mRNA fragments, using anti-m^7G antibody with preferential m^6Am demethylation by FTO (Sun et al., 2021). The method identified high-confidence m^6Am sites as well as the subset of m^6A sites located at the 5′UTR.

Mapping by RT signatures

Almost all high-throughput mapping methods of RNA modification involve the synthesis of cDNA by reverse transcriptases (RTases). Modifications that alter base pairing or affect RTase fidelity and processivity leave a trace in the cDNA, called RT signature, in the form of a typical mutation profile, premature RT terminations (steep drop in coverage), or a combination of the two (Figure 2B). Signature patterns may be enhanced by using specific RTases or under specific reaction conditions (Li et al., 2017). Detection of RT signatures on its own is often not enough for unequivocal mapping, and an enrichment step is usually required prior to cDNA synthesis.

(D) Mapping by differential enzymatic compatibility.
(E) Mapping by metabolic labeling.
(F) Mapping modifications by identifying the binding sites of their writers.
(G) Mapping modifications by direct RNA sequencing.

RT signatures can be simple or complex, consisting of a combination of RT arrest with a typical mismatch profile. For example, the RT signature of inosine, the product of adenosine-to-inosine (A-to-I) editing (Levanon et al., 2004; Li et al., 2009) is unambiguous. Unlike adenosine, inosine base pairs with cytidine (C) rather than uridine (U) resulting in U-to-C substitutions in the cDNA. During library preparation, these substitutions generate a typical adenosine-to-guanosine (A-to-G) RT signature (Levanon et al., 2004; Li et al., 2009). Although this signature is easily identified, low-stoichiometry sites may be falsely accounted as sequencing errors and escape detection. Additionally, single-nucleotide substitutions may be falsely identified as inosine sites.

m^1A RT signature is more complex. Under physiological conditions, m^1A has both a methyl group and a positive charge, which affect the fidelity and processivity of RT, resulting in misincorporation and premature terminations. Characterizing m^1A RT signatures in tRNA revealed that the nucleotide 3′ to m^1A affects misincorporation profile and RT arrest patterns (Hauenschild et al., 2015). Initially, two independent studies identified m^1A as an epitranscriptomic mark by MS and detected a large number of sites in mRNA using immunocapturing and NGS (Dominissini et al., 2016; Li et al., 2016). An improved protocol provided single-base resolution maps by using the thermostable group II intron reverse transcriptase (TGIRT) to amplify m^1A's RT signature (owing to TGIRT's higher processivity and increased misincorporation rate at m^1A sites, under tailored buffer conditions) (Li et al., 2017) Surprisingly, a similar approach taken by another group identified only a handful of m^1A sites in mRNA (Safra et al., 2017). How can the use of similar approaches lead to such divergent outcomes? The discrepancy, most likely, is due to differences in protocol conditions utilized by each group resulting in lower sensitivity of the latter study. These include competitive elution, tailored TGIRT buffer, validation by AlkB enzymatic demethylation, and the use of molecular indices (Li et al., 2017) compared to bulk extraction, commercial TGIRT buffer, m^1A-to-m^6A rearrangement, and no use of molecular indices (Safra et al., 2017), as well as major differences in the bioinformatic analysis.

The notion that RT signatures result from properties of both the modification and the RTase led to a novel approach for m^1A mapping. This method used an evolved RTase that can efficiently read-through m^1A sites while leaving a strong misincorporation signature. Hundreds of m^1A sites were mapped at single-base resolution, and their methylation stoichiometry was determined, validating previously identified sites (Zhou et al., 2019).

Mapping by differential chemical reactivity or enzymatic compatibility

In some cases, RNA modifications exhibit differential chemical reactivity which can be utilized for their mapping (Figure 2C). Ψ is the product of U isomerization, formed by a break of the nitrogen-carbon glycosidic bond between the base and the ribose, rotation of the base, and formation of a new bond. As Ψ is RT-silent and cannot be detected by sequencing alone, its mapping relies on its differential chemical reactivity with CMC (N-cyclohexyl-N′-(β-[N-methylmorpholino] ethyl) carbodiimide). U, G, and Ψ react with CMC; however, the reaction can be reversed for U and G but not for Ψ. Ψ-CMC adducts induce RT arrest one nucleotide downstream to the Ψ site. Based on this, several independent studies identified hundreds of Ψ sites in yeast and mammals, with very limited overlap between them (Carlile et al., 2015; Lovejoy et al., 2014; Schwartz et al., 2014). These methods suffer mainly from incomplete reaction with CMC and inability to pre-enrich Ψ sites, leading to inefficient Ψ detection. A more sensitive method combined click chemistry with a CMC analog and detected over a thousand sites in human and mouse mRNAs showing a more significant overlap with each of the previous studies (Li et al., 2015). Another approach, RBS-seq (RNA bisulfite sequencing), utilizes the differential chemical reactivity of Ψ under bisulfite treatment that forms a Ψ-monobisulfite adduct, erasing the CMC-RT arrest signature, thus allowing validation of modification sites (Khoddami et al., 2019). RBS-seq is not limited to Ψ mapping and can be used for transcriptome-wide sensitive and simultaneous detection of m^5C, Ψ, and m^1A at single-base resolution (Khoddami et al., 2019). Other modifications that can be mapped based on their differential chemical reactivity include m^5C (Janin et al., 2019; Squires et al., 2012), 7-methylguanosine (m^7G), and 3-methylcytidine (m^3C) (Marchand et al., 2018; Zhang et al., 2019).

Differential chemical reactivity may sometimes lead to differential enzymatic compatibility which can also be utilized for mapping. Methylation of the ribose at the 2′ position converts 2′-OH to 2′-*O*-methylated (2′-OMe) nucleotides (Nm), an abundant modification in different RNA species including rRNA, tRNA, snRNA, and microRNA. In mRNA, Nm is present both in the cap and in internal positions. Initially, mapping approaches of Nm were based on its property to pause RT when deoxyribonucleotide triphosphate amounts are limited, resulting in under-representation of Nm positions in the cDNA ends and providing a negative readout of Nm landscape (Maden et al., 1995). These methods were later coupled to NGS (Birkedal et al., 2015; Marchand et al., 2016; Gumienny et al., 2017; Incarnato et al., 2017; Krogh et al., 2017) but were unable to detect sites in mRNA due to the low abundance of specific transcripts and low stoichiometry. Two new approaches, Nm sequencing (Nm-seq) (Dai et al., 2017) and ribose oxidation sequencing (Zhu et al., 2017), took advantage of differential properties of 2′-OH and 2′-OMe nucleosides, both chemically and enzymatically (Figure 2D). Unlike unmodified 3′ ends of RNA fragments, 3′ Nm ends are resistant to periodate oxidation, allowing fragment shortening by iterative oxidation-elimination-dephosphorylation cycles, one base per cycle, until Nm is reached. The iterative exposure process results in enrichment of fragments ending with Nm. A final step of only oxidation and elimination generates two types of 3′ ends: 2′-OH and 2′-OMe, and only the latter is compatible for adaptor ligation and library preparation. Initially, the Nm-seq method suffered from a bias due to a mispriming artifact, resulting from RT primer annealing to short internal sequences and amplification of adaptor-unligated fragments during library preparation. This was later amended by improving the library preparation part of the protocol (Dai et al., 2018). As this approach requires iterative shortening of the RNA fragments, it is more efficient for mapping Nm sites in small RNAs (Hsu et al., 2019). The major limitations of these methods are the need for high input amounts and that they are time- and labor-consuming due to the need to perform iterative cycles for fragment shortening.

Improving mapping accuracy and resolution

The need for more accurate m^{6}A mapping tools with single-nucleotide resolution prompted the development of several new methods. m^{6}A-CLIP adopted the UV cross-linking and immunoprecipitation (CLIP) approach for antibody-enriched m^{6}A-modified RNA fragments, followed by proteinase K treatment to detect m^{6}A positions in mammalian mRNA at single-nucleotide precision, based on RT signatures (Ke et al., 2015). A slightly different method, PA-m^{6}A-seq (photo-crosslinking-assisted m^{6}A sequencing) identifies m^{6}A positions in antibody-enriched 4-thiouridine-labeled intact polyA+ RNA after cross-linking with 365 nm UV light. Proteinase K digestion prior to library preparation generates a typical RT signature of U-to-C substitutions in the sequence data (Chen et al., 2015). The CLIP approach was also used in miCLIP/miCLIP2 methods. The initial miCLIP protocol identified the RT signatures of different commercially available anti-m^{6}A antibodies (Linder et al., 2015). The improved miCLIP2 protocol uses mRNA from Mettl3 knockout (KO) cells, depleted from m^{6}A (Geula et al., 2015), combined with machine learning to reduce false-positive m^{6}A site detection (Körtel et al., 2021).

The need for quantitative m^{6}A mapping fueled the development of m^{6}A-LAIC-seq (m^{6}A-level and isoform-characterization sequencing), an isoform-aware mapping tool that assessed the stoichiometry of m^{6}A sites. This tool differs from typical antibody-based mapping as RNA is not fragmented, both antibody-bound and unbound fractions are sequenced, and methylated spike-in RNAs are added to the sample prior to enrichment. These adaptations allow to identify the methylation status of different transcript isoforms and to determine their methylation stoichiometry (Molinie et al., 2016). However, as transcripts often carry more than one m^{6}A site, the method defines the methylation stoichiometry at the transcript variant rather than the position levels.

Antibody cross-reactivity raised the need for the development of antibody-independent m^{6}A mapping methods. Two independent methods: MAZTER-seq (Garcia-Campos et al., 2019) and m^{6}A-REF-seq (Chen et al., 2021) used the m^{6}A-sensitive MazF RNase, which cleaves RNA only at unmethylated ACA sites, allowing the detection of m^{6}A sites at single-base resolution. Both methods provide both base resolution and site stoichiometry. However, they are limited to the subset of m^{6}A sites that occur in ACA-containing motifs (i.e., RRACA) and that are located within suitable distances of nearby ACA sequences. In addition, these methods are influenced by the amount of MazF used, as insufficient amounts may result in undigested modified sequences and false site detection. Classification of these sites into confidence groups, combined with a calculated m^{6}A-seq score, provided a strong orthogonal validation of the sites (Garcia-Campos et al., 2019). Calibration of m^{6}A mapping based on these sequence truncation approaches uses modification-free *in vitro* transcribed RNA as negative control to distinguish genuine sites from false positive ones (Zhang et al., 2021). Although the method was tested for calibrating mapping m^{6}A by MAZTER-seq and m^{5}C by BS-seq, the authors claim that the approach can be used for any mapping method (Zhang et al., 2021).

Mapping by metabolic and enzymatic labeling

Specific recognition is not limited to antibodies. Proteins such as readers or erasers also recognize and bind specific modifications and can be harnessed to guide transcript labeling at or next to a specific modification. Several mapping tools adopted this strategy for mapping m^{6}A:

DART-seq uses a fused protein consisting of APOBEC1, a C-to-U cytidine deaminase, with the YTH (YT512-B homology) domain of YTHDF2, an m^{6}A reader that recognizes and binds m^{6}A-modified RNA sequences, to induce C-to-U editing in the close proximity of m^{6}A sites. Similar to A-to-I editing, C-to-U deamination is easily recognized by a simple C-to-T RT signature (Meyer, 2019). The two main limitations of this approach are that binding specificity of YTHDF2 may be restricted to a subset of m^{6}A sites excluding sites in non-YTHDF2 targets and reduced sensitivity of the method for low-abundance and low-stoichiometry m^{6}A sites. A study recently published online describes the first method for transcriptome-wide m^{6}A mapping at single-cell resolution. The method, scDART-seq (single-cell DART-seq), couples the DART-seq approach with single-cell RNA-seq (using the droplet-based 10xGenomics and the SMART-seq2 platforms). scDART-seq identified thousands of m^{6}A sites, most of which occur only in a small proportion of cells (Tegowski et al., 2022).

The concept of targeting m^{6}A to induce a local detectable change in the transcript was also adopted by m^{6}A-SEAL-seq that uses FTO, an m^{6}A eraser. Here, labeling is based on the enzymatic activity of FTO, which oxidizes m^{6}A to generate a highly unstable product, N^6-hydroxymethyladenosine (hm^{6}A). Treatment of hm^{6}A with dithiothreitol (DTT) generates a significantly more stable product, N^6-dithiolsitolmethyladenosine (dm^{6}A), which contains a thiol group available for further labeling with biotin. Biotin-labeled RNA fragments are pulled down with streptavidin beads and sequenced (Wang et al., 2020). Although the method is sensitive, efficient, and antibody-independent, it does not provide a single-nucleotide resolution.

m^{6}A mapping can rely on metabolic labeling of RNA in living cells (Figure 2E) or *in vitro*. m^{6}A-label-seq is based on the fact that m^{6}A is formed by a reaction involving the transfer of a methyl group from S-adenosyl methionine (SAM) to an adenosine residue. Feeding cells with a methionine analog, Se-allyl-l-selenohomocysteine, which replaces the methyl group on SAM with an allyl group, results in the presence of N^6-allyladenosines (a^{6}A) at m^{6}A positions. a^{6}A can be identified by iodination-induced misincorporation RT signatures (Shu et al., 2020). Although m^{6}A-label-seq provides increased resolution compared to antibody-based mapping, Se-allyl-l-selenohomocysteine induces a stress response. Considering the dynamic nature of m^{6}A, such stress may alter m^{6}A levels and patterns (Shu et al., 2020).

Mapping modifications by identifying the binding sites of their writers

RNA modifications are installed by dedicated enzymes that work in a complex or as standalone enzymes. The interaction of writers with their target RNAs can be exploited to map the modified sites. This approach was used to map inosine according to the specific ADAR proteins that introduces

them. The method, irCLASH (infrared crosslinking, ligation, and sequencing of hybrids) identified site-specific editing of ADAR1 and ADAR2 (Song et al., 2020). A similar strategy used crosslinking and immunoprecipitation sequencing (CLIP-seq) to validate the Nm sites of different 2′-*O*-Methyltransferases in yeast mRNA (Bartoli et al., 2018). Mapping an RNA modification by identifying the targets of its writer enzyme (Figure 2F) can be useful in cases where there are no specific antibodies or known differential properties for the modification but its writer/s have been identified.

Mapping modifications by direct RNA sequencing

The Oxford Nanopore Technologies platform offers a direct method for RNA sequencing based on changes in the ionic current signal for each individual base (Figure 2G). During direct RNA sequencing, intact transcript molecules pass through a motor protein into membrane-embedded protein nanopores, which are coupled to highly sensitive sensor chips. Constant voltage is applied across the membrane and ionic current passes through the nanopores. When a nucleotide passes through a nanopore, it produces a distinctive and typical shift in the current. Base-calling relies on specific ion current changes, and detection of specific current shifts are used to determine and distinguish modified and unmodified nucleotides (Wang et al., 2021).

The large number of RNA modifications poses a challenge for their mapping, since base-calling relies on dedicated algorithms and machine learning, which are limited by the lack of RNA-modification standards (Alfonzo et al., 2021). In the last few years, integration of computational learning approaches, such as convolutional neural networks and recurrent neural networks (He et al., 2016; Cozzuto et al., 2020), significantly improved base-calling of direct RNA sequencing and detection of RNA modifications. Importantly, direct RNA sequencing does not require cDNA synthesis, RNA fragmentation, or amplification steps, and its further development is expected to significantly advance the epitranscriptomics field.

A recent study developed a computational method, xPore, for identifying m^6A sites in direct RNA sequencing data (Pratanwanich et al., 2021). Although xPore does not identify the type of modification at each position, the authors were able to restrict the analysis to a single modification by considering one-directional signal shifts. Xpore identified thousands of m^6A sites at base precision and determined their stoichiometry (Pratanwanich et al., 2021).

Choosing a method

As m^6A is the most abundant internal mRNA modification, it is also the most studied one. We outlined here the main m^6A mapping approaches, each with its advantages and drawbacks, raising the question of which method to choose. The answer depends on the biological system, the amount of input RNA available, and the needed resolution of mapped sites. For example, low-input methods will miss low-stoichiometry sites, and high amounts of input may not be available in all systems. Moreover, methods like m^6A-seq are robust and identify thousands of sites but are blind to stoichiometry and a transcript variant's identity, while m6A-LAIC-seq provides the methylation state of transcripts without identifying site position. Orthogonal mapping may provide high-confidence site detection but in return may result in a low number of sites identified by the different methods. This reflects once again need for a better mapping tool.

Validations

Inconsistencies between different mapping strategies, especially of low-abundance modifications, and their non-stoichiometric nature, particularly in cases where a specific position is modified in only a small fraction of the transcripts (low stoichiometry), accentuated the need for validation methods, both for the mapping method as well as for specific sites.

Validation of mapping method

Validation of the mapping method can be carried out by comparing mapping results to control matching samples exhibiting depleted and increased levels of the modification. Depleted samples set the baseline levels of the methods, while over-modified samples increase the confidence of site detection, especially in borderline-identified sites. There are two main approaches for obtaining such samples: depletion of RNA from a specific modification by enzymatic, chemical, or physical treatment can remove or convert an RNA modification. Such treatments are carried out *in vitro* on purified RNA and produce a matching sample with the same transcript composition but devoid of the modification. The limitation of such treatments is their effect on RNA integrity. m^1A, for example, can be enzymatically removed by treating the RNA sample with the bacterial AlkB enzyme, which can oxidatively remove the methyl group in an α-ketoglutarate and iron(II)-dependent reaction (Cozen et al., 2015). Alternatively, under alkaline conditions, m^1A can be converted into m^6A by Dimroth rearrangement (Macon and Wolfenden, 1968). Both treatments deplete m^1A from the RNA sample and were used to validate m^1A positions (Dominissini et al., 2016; Li et al., 2016; Li et al., 2017). However, removal of m^1A by AlkB treatment is more efficient as the alkaline conditions needed for Dimroth rearrangement led to excessive RNA degradation (Li et al., 2017).

Modification depletion can also be carried out by genetic manipulation through KO or knockdown (KD) of the relevant writers. Loss of sites in RNA from KO/KD cell models, when compared to control samples, confirms the validity of the sites identified. For example, KO of Mettl3, the main writer of m^6A, in mouse embryonic stem cells (mESCs) was used to validate m^6A site identification in mESCs (Geula et al., 2015). It should be taken into consideration that modification depletion through genetic manipulation may alter gene expression profiles.

Validation of specific sites

Detecting a specific modification in a site-specific manner can be performed by protection assays. In principle, these assays are not limited to a specific modification or transcript. The method protects a short sequence of interest from digestion by mung bean nuclease through annealing of a complementary oligonucleotide. The protected RNA fragments are purified and subjected to LC-MS/MS analysis to confirm the presence of the modification. The method was successfully used to establish a comprehensive modification profile of *Saccharomyces cerevisiae's* 18S and 25S rRNA (Yang et al., 2016).

Other available methods for site validation were developed specifically for m^{6}A:

The SCARLET (site-specific cleavage and radioactive-labeling followed by ligation-assisted extraction and thin-layer chromatography) method determines the exact position of an m^{6}A site and its methylation stoichiometry (Liu et al., 2013). This method may also validate RNA modifications other than m^{6}A, such as m^{5}C, Ψ, and Nm.

Harnessing CRISPR-based technologies offers another tool for site-specific validation. The method makes use of CRISPR-Cas9 fused to an eraser of a particular modification that is guided to a specific site by guide RNA to remove of the modification in that position. The method was successfully used by fusing CRISPR-Cas9 with the m^{6}A erasers ALKBH5 and FTO for site-specific m^{6}A demethylation (Liu et al., 2019).

Additional factors that should be taken into account when mapping RNA modifications include sequencing depth, dedicated bioinformatics tools, and the source of RNA sample (the choice of cell line/tissue and growth conditions that may enhance or reduce the number of sites identified). These factors differ according to the individual modification studied.

FUNCTIONAL CHARACTERIZATION

Understanding the roles of RNA modifications calls for their functional characterization in addition to their detection and mapping. Such characterization reveals the mechanisms by which a specific RNA modification acts in regulation of gene expression. While functional characterization of most mRNA modifications is still in an early phase, the information regarding m^{6}A roles is rapidly expanding. Identification of reader proteins was proved to be an important tool for deducing the regulatory roles of a modification and the cellular mechanisms involved. The initial discovery of dedicated m^{6}A-binding proteins, m^{6}A readers, (Dominissini et al., 2012) paved the way to uncovering the various m^{6}A functions and associated mechanisms exposing its regulatory roles. m^{6}A plays a role in a large number of processes both in the nucleus as well as in the cytoplasm.

In the nucleus, m^{6}A is involved in a number of cellular processes that regulate gene expression. These include chromosome X transcriptional silencing (Patil et al., 2016), activation of gene expression through methylation of chromatin-associated regulatory RNAs (Liu et al., 2020) and enhancer RNAs (Lee et al., 2021), R-loops resolution (Yang et al., 2019; Kang et al., 2021), alternative splicing and alternative polyadenylation (Xiao et al., 2016; Liu et al., 2015; Liu et al., 2017; Kasowitz et al., 2018), and nuclear export (Roundtree et al., 2017). However, regulation of gene expression by m^{6}A is not limited to nuclear processes. m^{6}A also plays a role in regulation of translation (Wang et al., 2015; Shi et al., 2017), localization of transcripts to stress granules (Anders et al., 2018), and RNA degradation (Wang et al., 2014; Du et al., 2016). The different roles are dictated by the reader protein that binds m^{6}A-methylated RNA to execute the specific regulatory role. Thus, identification of reader proteins is central for deducing the regulatory roles of a specific modification and the cellular mechanisms involved.

Strategies for identification of reader proteins

Several strategies can be adopted to identify reader proteins. Combining advanced MS profiling, NGS, and molecular biology approaches generated a set of tools for identification and characterization of reader proteins.

Identification of reader proteins, specific for known modified sequences, can be carried out by RNA affinity chromatography (RAC) assays coupled to MS. In this *in vitro* approach, immobilized pairs of RNA oligonucleotides, one of which is modified, are incubated with cell lysates. Bound proteins are pulled down and identified by LC-MS/MS. RAC experiments were used to identify the first m^{6}A readers: YTHDF2 and YTHDF3 (Dominissini et al., 2012), which were later shown to regulate RNA turnover (Wang et al., 2014) and translation (Wang et al., 2015).

Identifying the interactome of a given modification by global MS-based interaction screens for reader proteins allows the identification of both readers and RNA-binding proteins that have a preference for unmodified sequences (anti-readers). One method that combined photo-cross-linking and proteomics for profiling the interactome of an RNA modification took advantage of the high-efficiency diazirine-based RNA photo-cross-linking (Arguello et al., 2017). A second global approach used stable isotope labeling with amino acids in cell culture (SILAC)-based m^{6}A-RNA pull-downs (Edupuganti et al., 2017). Both methods used MS analyses to characterize the m^{6}A interactome, reaching similar results. These independent studies identified novel m^{6}A anti-reader proteins G3BP1/2, USP10, CAPRIN1, and RBM42 as well as known m^{6}A readers (Arguello et al., 2017; Edupuganti et al., 2017).

Study the global effects of a given modification

The roles of mRNA modifications in regulation of gene expression were studied extensively in the past decade. These roles may be correlated with altered modification profiles in response to changing cellular conditions. To infer regulatory functions to a specific RNA modification, conditions of high and low levels of the modification (termed here as differential conditions) should be established. These may result from specific growth or stress conditions or from genetic manipulation of the modification's writers and erasers by KD, KO, or overexpression.

Once differential conditions are identified, profiling different parameters of RNA metabolism may highlight the affected mechanisms. These parameters may include global gene expression levels, RNA processing patterns, nuclear export, retention and transcript localization in the cytoplasm, RNA stability and degradation rates, ribosomal profiling, and translation efficiency of modified transcripts and differential protein expression levels, especially of modified transcripts. Correlation of modification maps with the above listed profiles may expose the molecular mechanisms associated with the modification.

For example, depletion of Mettl3, the catalytic unit of the m^{6}A writer complex, in mESCs resulted in altered splicing patterns and increased transcript stability of pluripotency genes, leading to differentiation arrest and embryonic lethality (Geula et al., 2015). While using genetically modified KO cell models often

produces a sharper outlining of the affected mechanisms, some modifications are essential and their depletion (by KO/KD of their writers) leads to cell death. KO of Mettl3, for instance, induces apoptosis in all differentiated cells excluding naive mESCs (Geula et al., 2015).

However, as mentioned above, unlike m^{6}A that is installed by a complex that is dedicated to mRNA and lncRNA, writing machineries of other mRNA modifications are more redundant in terms of substrate preference, acting on abundant noncoding RNAs (tRNA/rRNA/snRNA) as well as mRNA, making it complicated to restrict the KD/KO effect to the regulatory role of the modification in mRNA alone (Schaefer, 2021).

Study the effects on innate immunity

RNA modifications play important roles in the regulation of the antiviral innate immune response by controlling the recognition of viral RNAs and modulating the expression of both viral and antiviral genes. Effective triggering of this response relies on recognition of viral pathogens through activation of dedicated proteins such as RIG-I and MDA5. Pathogen-associated molecular patterns such as cytosolic double-stranded RNAs are recognized by RIG-I and MDA5 as non-self RNAs, leading to their activation, initiating a signaling cascade that results in the expression of antiviral genes including cytokines such as type I and III interferons (IFNs) (Thompson et al., 2021).

To study the effect of a given modification of the innate immune response, it is important to manipulate the modification's levels and monitor its effect on the cell's response to viral infection by determining viral RNA levels, as well as viral and host gene expression profiles. For example, internal m^{6}A modifications on viral RNA inhibit its recognition and binding by RIG-I. Upon viral infection, METTL3 translocates from the nucleus to the cytoplasm and installs m^{6}A on cytosolic viral RNAs. m^{6}A was shown to induce restructuring of the viral RNA and impair its recognition by RIG-I and MDA5 (Qiu et al., 2021). However, the role of m^{6}A in innate immunity is not confined to marking viral RNA and preventing RIG-I activation. During viral infection, transcripts of signaling proteins such as MAVS, TRAF3, and TRAF6, which are important for IFN induction, are demethylated by ALKBH5, leading to their retention in the nucleus and resulting in their reduced expression (Zheng et al., 2017).

The effect of RNA modifications on innate immunity is beyond their physiological context. A study in 2005 showed that RNA modifications such as Ψ and m^{5}C inhibit the innate immune response (Karikó et al., 2005). Follow-up studies showed that synthetic transcripts containing N^1-methylpseudouridine (m^{1}Ψ) increase protein synthesis and reduce the induction of the innate immune response through decreasing TLR3 activation (Andries et al., 2015). These studies led the way for the development of mRNA vaccines, a novel therapeutic approach, which was approved for use against the severe acute respiratory syndrome coronavirus 2 during the coronavirus disease 2019 pandemic (Nance and Meier, 2021).

The regulation of innate immunity by RNA modifications has been the focus of numerous studies and reviews (such as Thompson et al., 2021; Villanueva et al., 2020) and is beyond the scope of this technical primer.

Deducing affected mechanisms by reader manipulation

Reader proteins play essential roles in deciphering and executing the regulatory functions encoded by RNA modification through their exclusive interaction with modified target RNAs. Genetic manipulation of reader proteins was used to expose the regulatory gene expression mechanism governed by the modification. Rescue of the deletion phenotype with an active but not with an inactive reader further supports the identified functions.

Several regulatory roles of m^{6}A were identified by genetic manipulation of its reader proteins. For example, YTHDF2 KD led to prolonged half-life values of its m^{6}A-methylated mRNA target transcripts, and overexpression of YTHDF2 resulted in reduced m^{6}A mRNA levels, uncovering the role of m^{6}A in RNA degradation (Wang et al., 2014). The role of YTHDF2 in RNA degradation was further characterized showing that it is responsible for direct recruitment of the CCR4-NOT deadenylase complex to m^{6}A-decorated transcripts leading to their degradation (Du et al., 2016).

RNA restructuring

Unlike DNA, RNA is a single-strand molecule that folds into intricate structures, enabling its biological functions. RNA folding may expose or hide sequence motifs that mediate binding of dedicated RNA-binding proteins. RNA modifications can modulate RNA-protein interactions directly, through dedicated structures in the protein that recognize and bind modified sequences, or indirectly, by inducing different RNA folding in their vicinity, leading to restructuring and exposing sequence motifs, otherwise unavailable for protein binding. For example, YTH domain-containing proteins directly bind m^{6}A-modified sequences through a conserved aromatic cage structure (Luo and Tong, 2014). In contrast, the m^{6}A-dependent RNA binding mode of several heterogeneous nuclear ribonucleoproteins (hnRNPs) relies on m^{6}A-induced RNA structure alterations that expose their binding motifs, which are not necessarily methylated. This indirect binding mechanism, coined m^{6}A-switch, modulates the binding capacity of the m^{6}A readers HNRNPC (Liu et al., 2015) and HNRNPG (Liu et al., 2017).

In the past decade, many high-throughput methods for detecting the RNA structurome (structure of the cell transcriptome) were developed. These methods use different chemical reagents for determining the single- and double-strand sequences of the RNA *in vitro* and *in vivo* for structure analyses (Lu and Chang, 2016; Mitchell et al., 2019). Two chemical probes are widely used for *in vivo* transcriptome-wide mapping of the RNA structurome: dimethyl sulfate (DMS), which acts mostly on the Hoogsteen face of bases and is used in methods such as DMS-MaPseq (Zubradt et al., 2017), and SHAPE, which labels the 2'-OH of the ribose instead of the bases (Mustoe et al., 2018; Weeks, 2021). While both methods are efficient, there is still much room for improvement, especially since high concentrations of DMS are toxic and SHAPE molecules are hydrolytically unstable. A recent approach for transcriptome-wide RNA structure mapping, Keth-seq, uses a new labeling reagent, N3-kethoxal, that reversibly labels single-strand RNA *in vivo* under mild conditions. N3-kethoxal labeling induces RT arrest signatures. Removing the labeling erases the

RT signature to produce a control sample for validation (Weng et al., 2020).

Conducting global RNA structure analysis under differential conditions of a specific RNA modification and integrating the data with modification profiles may uncover its effects on RNA restructuring.

CONCLUDING REMARKS

The rapid expansion of the field of epitranscriptomics generated a large collection of tools for the detection, mapping, and functional characterization of both high- and low-abundance RNA modifications. Yet, despite the large arsenal of tools and strategies presented here, the field still needs comprehensive technologies to expand our knowledge of epitranscriptomic regulation of gene expression. The current major challenge in the field is the development of accurate, direct, modification-sensitive high-throughput RNA sequencing technology (Alfonzo et al., 2021). Perfecting the mapping tools, in terms of single-base-, single transcript-, and single cell-resolution; stoichiometry; input amounts; and reduced false site detection, is essential for bridging knowledge gaps in the field. The multitude of modifications in RNA molecules present another challenge: parallel mapping of different modifications in single transcripts, aiming to decipher combinatorial ''code'' analogous to the putative histone code. Moreover, the knowledge regarding the writers, readers, and erasers of several low-abundance mRNA modifications is still lacking, hindering their study and understanding. Meeting these challenges is expected to advance our knowledge of the multiple regulatory roles played by RNA modifications. Finally, the rapid development of epitranscriptomics modulating therapies make the advance of a better toolbox a major challenge in the coming years.

ACKNOWLEDGMENTS

The authors thank the Kahn Family Foundation for continuous support of their research. D.D. is supported by grants from the Israel Science Foundation (2494/18 and 2625/17) and the Human Frontier Science Program (CDA 00048/2018). G.R is supported by the European Research Council (ERC) under the European Union's Horizon 2020 research and innovation program (grant agreement no. 743168) and the Flight Attendant Medical Research Institute (FAMRI). G.R. and D.D. are supported by the German-Israeli Project Cooperation (DIP) of the German Federal Ministry of Education and Research and by a grant from the Varda and Boaz Dotan Research Center in Hemato-Oncology, Tel Aviv University. G.R. holds the Djerassi Chair in Oncology at the Tel Aviv University.

DECLARATION OF INTERESTS

The authors declare no competing interests.

REFERENCES

Akichika, S., Hirano, S., Shichino, Y., Suzuki, T., Nishimasu, H., Ishitani, R., Sugita, A., Hirose, Y., Iwasaki, S., Nureki, O., and Suzuki, T. (2019). Cap-specific terminal N^6-methylation of RNA by an RNA polymerase II-associated methyltransferase. Science *363*, eaav0080.

Alfonzo, J.D., Brown, J.A., Byers, P.H., Cheung, V.G., Maraia, R.J., and Ross, R.L. (2021). A call for direct sequencing of full-length RNAs to identify all modifications. Nat. Genet. *53*, 1113–1116.

Anders, M., Chelysheva, I., Goebel, I., Trenkner, T., Zhou, J., Mao, Y., Verzini, S., Qian, S.B., and Ignatova, Z. (2018). Dynamic m6A methylation facilitates mRNA triaging to stress granules. Life Sci. Alliance *1*, e201800113.

Andries, O., Mc Cafferty, S., De Smedt, S.C., Weiss, R., Sanders, N.N., and Kitada, T. (2015). N(1)-methylpseudouridine-incorporated mRNA outperforms pseudouridine-incorporated mRNA by providing enhanced protein expression and reduced immunogenicity in mammalian cell lines and mice. J. Control. Release *217*, 337–344.

Arango, D., Sturgill, D., Alhusaini, N., Dillman, A.A., Sweet, T.J., Hanson, G., Hosogane, M., Sinclair, W.R., Nanan, K.K., Mandler, M.D., et al. (2018). Acetylation of cytidine in mRNA promotes translation efficiency. Cell *175*, 1872–1886.e24.

Arguello, A.E., DeLiberto, A.N., and Kleiner, R.E. (2017). RNA chemical proteomics reveals the N6-methyladenosine (m6A)-regulated protein–RNA interactome. J. Am. Chem. Soc. *139*, 17249–17252.

Bartoli, K.M., Schaening, C., Carlile, T.M., and Gilbert, W.V. (2018). Conserved methyltransferase Spb1 targets mRNAs for regulated modification with 2′-O-methyl ribose. Preprint at bioRxiv. https://doi.org/10.1101/271916.

Basanta-Sanchez, M., Temple, S., Ansari, S.A., D'Amico, A., and Agris, P.F. (2016). Attomole quantification and global profile of RNA modifications: Epitranscriptome of human neural stem cells. Nucleic Acids Res. *44*, e26, e26.

Birkedal, U., Christensen-Dalsgaard, M., Krogh, N., Sabarinathan, R., Gorodkin, J., and Nielsen, H. (2015). Profiling of ribose methylations in RNA by high-throughput sequencing. Angew. Chem. Int. Ed. Engl. *54*, 451–455.

Boccaletto, P., Machnicka, M.A., Purta, E., Piątkowski, P., Bagiński, B., Wirecki, T.K., de Crécy-Lagard, V., Ross, R., Limbach, P.A., Kotter, A., et al. (2018). MODOMICS: a database of RNA modification pathways. 2017 update. Nucleic Acids Res. *46* (D1), D303–D307.

Carlile, T.M., Rojas-Duran, M.F., and Gilbert, W.V. (2015). Pseudo-Seq: genome-wide detection of pseudouridine modifications in RNA. Methods Enzymol. *560*, 219–245.

Chen, K., Lu, Z., Wang, X., Fu, Y., Luo, G.Z., Liu, N., Han, D., Dominissini, D., Dai, Q., Pan, T., and He, C. (2015). High-resolution N^6-methyladenosine (m^6A) map using photo-crosslinking-assisted m^6A sequencing. Angew Chem Int Ed Engl. *54*, 1587–1590.

Chen, H.X., Zhang, Z., Ma, D.Z., Chen, L.Q., and Luo, G.Z. (2021). Mapping single-nucleotide m6A by m6A-REF-seq. Methods. https://doi.org/10.1016/j.ymeth.2021.06.013.

Cozen, A.E., Quartley, E., Holmes, A.D., Hrabeta-Robinson, E., Phizicky, E.M., and Lowe, T.M. (2015). ARM-seq: AlkB-facilitated RNA methylation sequencing reveals a complex landscape of modified tRNA fragments. Nat. Methods *12*, 879–884.

Cozzuto, L., Liu, H., Pryszcz, L.P., Pulido, T.H., Delgado-Tejedor, A., Ponomarenko, J., and Novoa, E.M. (2020). Masterofpores: A workflow for the analysis of Oxford nanopore direct RNA sequencing datasets. Front. Genet. *11*, 211.

Dai, Q., Moshitch-Moshkovitz, S., Han, D., Kol, N., Amariglio, N., Rechavi, G., Dominissini, D., and He, C. (2017). Nm-seq maps 2′-O-methylation sites in human mRNA with base precision. Nat. Methods *14*, 695–698.

Dai, Q., Moshitch-Moshkovitz, S., Han, D., Kol, N., Amariglio, N., Rechavi, G., Dominissini, D., and He, C. (2018). Corrigendum: Nm-seq maps 2′-*O*-methylation sites in human mRNA with base precision. Nat. Methods *15*, 226–227.

Delatte, B., Wang, F., Ngoc, L.V., Collignon, E., Bonvin, E., Deplus, R., Calonne, E., Hassabi, B., Putmans, P., Awe, S., et al. (2016). RNA biochemistry. Transcriptome-wide distribution and function of RNA hydroxymethylcytosine. Science *351*, 282–285.

Desrosiers, R., Friderici, K., and Rottman, F. (1974). Identification of methylated nucleosides in messenger RNA from Novikoff hepatoma cells. Proc. Natl. Acad. Sci. USA *71*, 3971–3975.

Dominissini, D., and Rechavi, G. (2017). Loud and clear epitranscriptomic m1A signals: now in single-base resolution. Mol. Cell *68*, 825–826.

Dominissini, D., Moshitch-Moshkovitz, S., Schwartz, S., Salmon-Divon, M., Ungar, L., Osenberg, S., Cesarkas, K., Jacob-Hirsch, J., Amariglio, N., Kupiec,

M., et al. (2012). Topology of the human and mouse m6A RNA methylomes revealed by m6A-seq. Nature *485*, 201–206.

Dominissini, D., Moshitch-Moshkovitz, S., Salmon-Divon, M., Amariglio, N., and Rechavi, G. (2013). Transcriptome-wide mapping of N(6)-methyladenosine by m(6)A-seq based on immunocapturing and massively parallel sequencing. Nat. Protoc. *8*, 176–189.

Dominissini, D., Nachtergaele, S., Moshitch-Moshkovitz, S., Peer, E., Kol, N., Ben-Haim, M.S., Dai, Q., Di Segni, A., Salmon-Divon, M., Clark, W.C., et al. (2016). The dynamic N(1)-methyladenosine methylome in eukaryotic messenger RNA. Nature *530*, 441–446.

Du, H., Zhao, Y., He, J., Zhang, Y., Xi, H., Liu, M., Ma, J., and Wu, L. (2016). YTHDF2 destabilizes m(6)A-containing RNA through direct recruitment of the CCR4-NOT deadenylase complex. Nat. Commun. *7*, 12626.

Edupuganti, R.R., Geiger, S., Lindeboom, R.G.H., Shi, H., Hsu, P.J., Lu, Z., Wang, S.Y., Baltissen, M.P.A., Jansen, P.W.T.C., Rossa, M., et al. (2017). N^6-methyladenosine (m^6A) recruits and repels proteins to regulate mRNA homeostasis. Nat. Struct. Mol. Biol. *24*, 870–878.

Esteve-Puig, R., Bueno-Costa, A., and Esteller, M. (2020). Writers, readers and erasers of RNA modifications in cancer. Cancer Lett. *474*, 127–137.

Galloway, A., Atrih, A., Grzela, R., Darzynkiewicz, E., Ferguson, M.A.J., and Cowling, V.H. (2020). CAP-MAP: cap analysis protocol with minimal analyte processing, a rapid and sensitive approach to analysing mRNA cap structures. Open Biol. *10*, 190306.

Garcia-Campos, M.A., Edelheit, S., Toth, U., Safra, M., Shachar, R., Viukov, S., Winkler, R., Nir, R., Lasman, L., Brandis, A., et al. (2019). Deciphering the "m6A code" via antibody-independent quantitative profiling. Cell *178*, 731–747.e16.

Geula, S., Moshitch-Moshkovitz, S., Dominissini, D., Mansour, A.A., Kol, N., Salmon-Divon, M., Hershkovitz, V., Peer, E., Mor, N., Manor, Y.S., et al. (2015). Stem cells. m6A mRNA methylation facilitates resolution of naïve pluripotency toward differentiation. Science *347*, 1002–1006.

Gumienny, R., Jedlinski, D.J., Schmidt, A., Gypas, F., Martin, G., Vina-Vilaseca, A., and Zavolan, M. (2017). High-throughput identification of C/D box snoRNA targets with CLIP and RiboMeth-seq. Nucleic Acids Res. *45*, 2341–2353.

Hauenschild, R., Tserovski, L., Schmid, K., Thüring, K., Winz, M.L., Sharma, S., Entian, K.D., Wacheul, L., Lafontaine, D.L., Anderson, J., et al. (2015). The reverse transcription signature of N-1-methyladenosine in RNA-Seq is sequence dependent. Nucleic Acids Res. *43*, 9950–9964.

He, K., Zhang, X., Ren, S., and Sun, J. (2016). Deep residual learning for image recognition. Proceedings of the IEEE conference on computer vision and pattern recognition (IEEE), 770–778.

Hsu, P.J., Fei, Q., Dai, Q., Shi, H., Dominissini, D., Ma, L., and He, C. (2019). Single base resolution mapping of 2′-O-methylation sites in human mRNA and in 3′ terminal ends of small RNAs. Methods *156*, 85–90.

Incarnato, D., Anselmi, F., Morandi, E., Neri, F., Maldotti, M., Rapelli, S., Parlato, C., Basile, G., and Oliviero, S. (2017). High-throughput single-base resolution mapping of RNA 2′-O-methylated residues. Nucleic Acids Res. *45*, 1433–1441.

Janin, M., Ortiz-Barahona, V., de Moura, M.C., Martínez-Cardús, A., Llinàs-Arias, P., Soler, M., Nachmani, D., Pelletier, J., Schumann, U., Calleja-Cervantes, M.E., et al. (2019). Epigenetic loss of RNA-methyltransferase NSUN5 in glioma targets ribosomes to drive a stress adaptive translational program. Acta Neuropathol. *138*, 1053–1074.

Kang, H.J., Cheon, N.Y., Park, H., Jeong, G.W., Ye, B.J., Yoo, E.J., Lee, J.H., Hur, J.H., Lee, E.A., Kim, H., et al. (2021). TonEBP recognizes R-loops and initiates m6A RNA methylation for R-loop resolution. Nucleic Acids Res. *49*, 269–284.

Karikó, K., Buckstein, M., Ni, H., and Weissman, D. (2005). Suppression of RNA recognition by Toll-like receptors: the impact of nucleoside modification and the evolutionary origin of RNA. Immunity *23*, 165–175.

Kasowitz, S.D., Ma, J., Anderson, S.J., Leu, N.A., Xu, Y., Gregory, B.D., Schultz, R.M., and Wang, P.J. (2018). Nuclear m6A reader YTHDC1 regulates alternative polyadenylation and splicing during mouse oocyte development. PLoS Genet. *14*, e1007412.

Ke, S., Alemu, E.A., Mertens, C., Gantman, E.C., Fak, J.J., Mele, A., Haripal, B., Zucker-Scharff, I., Moore, M.J., Park, C.Y., et al. (2015). A majority of m6A residues are in the last exons, allowing the potential for 3′ UTR regulation. Genes Dev. *29*, 2037–2053.

Keith, G. (1995). Mobilities of modified ribonucleotides on two-dimensional cellulose thin-layer chromatography. Biochimie *77*, 142–144.

Khoddami, V., Yerra, A., Mosbruger, T.L., Fleming, A.M., Burrows, C.J., and Cairns, B.R. (2019). Transcriptome-wide profiling of multiple RNA modifications simultaneously at single-base resolution. Proc. Natl. Acad. Sci. USA *116*, 6784–6789.

Körtel, N., Rücklé, C., Zhou, Y., Busch, A., Hoch-Kraft, P., Sutandy, R.F., Haase, J., Pradhan, M., Musheev, M., Ostareck, D., Ostareck-Lederer, A., et al. (2021). Deep and accurate detection of m6A RNA modifications using miCLIP2 and m6Aboost machine learning. Nucleic Acids Res. *49*, e92.

Krogh, N., Birkedal, U., and Nielsen, H. (2017). RiboMeth-seq: Profiling of 2′-O-Me in RNA. Methods Mol. Biol. *1562*, 189–209.

Lauman, R., and Garcia, B.A. (2020). Unraveling the RNA modification code with mass spectrometry. Mol. Omics *16*, 305–315.

Lee, J.H., Wang, R., Xiong, F., Krakowiak, J., Liao, Z., Nguyen, P.T., Moroz-Omori, E.V., Shao, J., Zhu, X., Bolt, M.J., et al. (2021). Enhancer RNA m6A methylation facilitates transcriptional condensate formation and gene activation. Mol. Cell *81*, 3368–3385.e9.

Levanon, E.Y., Eisenberg, E., Yelin, R., Nemzer, S., Hallegger, M., Shemesh, R., Fligelman, Z.Y., Shoshan, A., Pollock, S.R., Sztybel, D., et al. (2004). Systematic identification of abundant A-to-I editing sites in the human transcriptome. Nat. Biotechnol. *22*, 1001–1005.

Li, S., and Limbach, P.A. (2012). Method for comparative analysis of ribonucleic acids using isotope labeling and mass spectrometry. Anal. Chem. *84*, 8607–8613.

Li, J.B., Levanon, E.Y., Yoon, J.K., Aach, J., Xie, B., Leproust, E., Zhang, K., Gao, Y., and Church, G.M. (2009). Genome-wide identification of human RNA editing sites by parallel DNA capturing and sequencing. Science *324*, 1210–1213.

Li, X., Zhu, P., Ma, S., Song, J., Bai, J., Sun, F., and Yi, C. (2015). Chemical pulldown reveals dynamic pseudouridylation of the mammalian transcriptome. Nat. Chem. Biol. *11*, 592–597.

Li, X., Xiong, X., Wang, K., Wang, L., Shu, X., Ma, S., and Yi, C. (2016). Transcriptome-wide mapping reveals reversible and dynamic N(1)-methyladenosine methylome. Nat. Chem. Biol. *12*, 311–316.

Li, X., Xiong, X., Zhang, M., Wang, K., Chen, Y., Zhou, J., Mao, Y., Lv, J., Yi, D., Chen, X.W., et al. (2017). Base-Resolution Mapping Reveals Distinct m1A Methylome in Nuclear- and Mitochondrial-Encoded Transcripts. Mol. Cell *68*, 993–1005.e9.

Linder, B., Grozhik, A.V., Olarerin-George, A.O., Meydan, C., Mason, C.E., and Jaffrey, S.R. (2015). Single-nucleotide-resolution mapping of m6A and m6Am throughout the transcriptome. Nat. Methods *12*, 767–772.

Liu, N., Parisien, M., Dai, Q., Zheng, G., He, C., and Pan, T. (2013). Probing N6-methyladenosine RNA modification status at single nucleotide resolution in mRNA and long noncoding RNA. RNA *19*, 1848–1856.

Liu, N., Dai, Q., Zheng, G., He, C., Parisien, M., and Pan, T. (2015). N(6)-methyladenosine-dependent RNA structural switches regulate RNA-protein interactions. Nature *518*, 560–564.

Liu, N., Zhou, K.I., Parisien, M., Dai, Q., Diatchenko, L., and Pan, T. (2017). N6-methyladenosine alters RNA structure to regulate binding of a low-complexity protein. Nucleic Acids Res. *45*, 6051–6063.

Liu, X.M., Zhou, J., Mao, Y., Ji, Q., and Qian, S.B. (2019). Programmable RNA N^6-methyladenosine editing by CRISPR-Cas9 conjugates. Nat. Chem. Biol. *15*, 865–871.

Liu, J., Dou, X., Chen, C., Chen, C., Liu, C., Xu, M.M., Zhao, S., Shen, B., Gao, Y., Han, D., and He, C. (2020). *N* ^{6}-methyladenosine of chromosome-associated regulatory RNA regulates chromatin state and transcription. Science *367*, 580–586.

Lovejoy, A.F., Riordan, D.P., and Brown, P.O. (2014). Transcriptome-wide mapping of pseudouridines: pseudouridine synthases modify specific mRNAs in S. cerevisiae. PLoS ONE *9*, e110799.

Lu, Z., and Chang, H.Y. (2016). Decoding the RNA structurome. Curr. Opin. Struct. Biol. *36*, 142–148.

Luo, S., and Tong, L. (2014). Molecular basis for the recognition of methylated adenines in RNA by the eukaryotic YTH domain. Proc. Natl. Acad. Sci. USA *111*, 13834–13839.

Ma, H., Wang, X., Cai, J., Dai, Q., Natchiar, S.K., Lv, R., Chen, K., Lu, Z., Chen, H., Shi, Y.G., et al. (2019). N^{6-}Methyladenosine methyltransferase ZCCHC4 mediates ribosomal RNA methylation. Nat. Chem. Biol. *15*, 88–94.

Macon, J.B., and Wolfenden, R. (1968). 1-Methyladenosine. Dimroth rearrangement and reversible reduction. Biochemistry *7*, 3453–3458.

Maden, B.E.H., Corbett, M.E., Heeney, P.A., Pugh, K., and Ajuh, P.M. (1995). Classical and novel approaches to the detection and localization of the numerous modified nucleotides in eukaryotic ribosomal RNA. Biochimie *77*, 22–29.

Marchand, V., Blanloeil-Oillo, F., Helm, M., and Motorin, Y. (2016). Illumina-based RiboMethSeq approach for mapping of 2′-O-Me residues in RNA. Nucleic Acids Res. *44*, e135.

Marchand, V., Ayadi, L., Ernst, F.G.M., Hertler, J., Bourguignon-Igel, V., Galvanin, A., Kotter, A., Helm, M., Lafontaine, D.L.J., and Motorin, Y. (2018). AlkAniline-Seq: Profiling of m^7 G and m^3 C RNA Modifications at Single Nucleotide Resolution. Angew. Chem. Int. Ed. Engl. *57*, 16785–16790.

Mauer, J., Luo, X., Blanjoie, A., Jiao, X., Grozhik, A.V., Patil, D.P., Linder, B., Pickering, B.F., Vasseur, J.J., Chen, Q., et al. (2017). Reversible methylation of m^6A_m in the 5′ cap controls mRNA stability. Nature *541*, 371–375.

Meyer, K.D. (2019). DART-seq: an antibody-free method for global m^6A detection. Nat. Methods *16*, 1275–1280.

Meyer, K.D., Saletore, Y., Zumbo, P., Elemento, O., Mason, C.E., and Jaffrey, S.R. (2012). Comprehensive analysis of mRNA methylation reveals enrichment in 3′ UTRs and near stop codons. Cell *149*, 1635–1646.

Mitchell, D., 3rd, Assmann, S.M., and Bevilacqua, P.C. (2019). Probing RNA structure in vivo. Curr. Opin. Struct. Biol. *59*, 151–158.

Molinie, B., Wang, J., Lim, K.S., Hillebrand, R., Lu, Z.X., Van Wittenberghe, N., Howard, B.D., Daneshvar, K., Mullen, A.C., Dedon, P., et al. (2016). m(6)A-LAIC-seq reveals the census and complexity of the m(6)A epitranscriptome. Nat. Methods *13*, 692–698.

Mustoe, A.M., Busan, S., Rice, G.M., Hajdin, C.E., Peterson, B.K., Ruda, V.M., Kubica, N., Nutiu, R., Baryza, J.L., and Weeks, K.M. (2018). Pervasive regulatory functions of mRNA structure revealed by high-resolution SHAPE probing. Cell *173*, 181–195.e18.

Nance, K.D., and Meier, J.L. (2021). Modifications in an Emergency: The Role of N1-Methylpseudouridine in COVID-19 Vaccines. ACS Cent. Sci. *7*, 748–756.

Patil, D.P., Chen, C.K., Pickering, B.F., Chow, A., Jackson, C., Guttman, M., and Jaffrey, S.R. (2016). m(6)A RNA methylation promotes XIST-mediated transcriptional repression. Nature *537*, 369–373.

Paulines, M.J., and Limbach, P.A. (2017). Stable isotope labeling for improved comparative analysis of RNA digests by mass spectrometry. J. Am. Soc. Mass Spectrom. *28*, 551–561.

Pratanwanich, P.N., Yao, F., Chen, Y., Koh, C.W.Q., Wan, Y.K., Hendra, C., Poon, P., Goh, Y.T., Yap, P.M.L., Chooi, J.Y., et al. (2021). Identification of differential RNA modifications from nanopore direct RNA sequencing with xPore. Nat. Biotechnol. *39*, 1394–1402.

Qiu, W., Zhang, Q., Zhang, R., Lu, Y., Wang, X., Tian, H., Yang, Y., Gu, Z., Gao, Y., Yang, X., Cui, G., et al. (2021). N 6-methyladenosine RNA modification suppresses antiviral innate sensing pathways via reshaping double-stranded RNA. Nat. Commun. *12*, 1582.

Roundtree, I.A., Luo, G.Z., Zhang, Z., Wang, X., Zhou, T., Cui, Y., Sha, J., Huang, X., Guerrero, L., Xie, P., et al. (2017). YTHDC1 mediates nuclear export of N^6-methyladenosine methylated mRNAs. eLife *6*, e31311.

Safra, M., Sas-Chen, A., Nir, R., Winkler, R., Nachshon, A., Bar-Yaacov, D., Erlacher, M., Rossmanith, W., Stern-Ginossar, N., and Schwartz, S. (2017). The m1A landscape on cytosolic and mitochondrial mRNA at single-base resolution. Nature *551*, 251–255.

Sarin, L.P., Kienast, S.D., Leufken, J., Ross, R.L., Dziergowska, A., Debiec, K., Sochacka, E., Limbach, P.A., Fufezan, C., Drexler, H.C.A., and Leidel, S.A. (2018). Nano LC-MS using capillary columns enables accurate quantification of modified ribonucleosides at low femtomol levels. RNA *24*, 1403–1417.

Schaefer, M.R. (2021). The Regulation of RNA Modification Systems: The Next Frontier in Epitranscriptomics? Genes (Basel) *12*, 345.

Schwartz, S., Bernstein, D.A., Mumbach, M.R., Jovanovic, M., Herbst, R.H., León-Ricardo, B.X., Engreitz, J.M., Guttman, M., Satija, R., Lander, E.S., et al. (2014). Transcriptome-wide mapping reveals widespread dynamic-regulated pseudouridylation of ncRNA and mRNA. Cell *159*, 148–162.

Shi, H., Wang, X., Lu, Z., Zhao, B.S., Ma, H., Hsu, P.J., Liu, C., and He, C. (2017). YTHDF3 facilitates translation and decay of N^6-methyladenosine-modified RNA. Cell Res. *27*, 315–328.

Shu, X., Cao, J., Cheng, M., Xiang, S., Gao, M., Li, T., Ying, X., Wang, F., Yue, Y., and Lu, Z. (2020). A metabolic labeling method detects m6A transcriptome-wide at single base resolution. Nat. Chem. Biol. *16*, 887–895.

Solivio, B., Yu, N., Addepalli, B., and Limbach, P.A. (2018). Improving RNA modification mapping sequence coverage by LC-MS through a nonspecific RNase U2-E49A mutant. Anal. Chim. Acta *1036*, 73–79.

Song, Y., Yang, W., Fu, Q., Wu, L., Zhao, X., Zhang, Y., and Zhang, R. (2020). irCLASH reveals RNA substrates recognized by human ADARs. Nat. Struct. Mol. Biol. *27*, 351–362.

Squires, J.E., Patel, H.R., Nousch, M., Sibbritt, T., Humphreys, D.T., Parker, B.J., Suter, C.M., and Preiss, T. (2012). Widespread occurrence of 5-methylcytosine in human coding and non-coding RNA. Nucleic Acids Res. *40*, 5023–5033.

Stacey, K.A. (1965). Intracellular modification of nucleic acids. Br. Med. Bull. *21*, 211–216.

Su, D., Chan, C.T., Gu, C., Lim, K.S., Chionh, Y.H., McBee, M.E., Russell, B.S., Babu, I.R., Begley, T.J., and Dedon, P.C. (2014). Quantitative analysis of ribonucleoside modifications in tRNA by HPLC-coupled mass spectrometry. Nat. Protoc. *9*, 828–841.

Sun, H., Zhang, M., Li, K., Bai, D., and Yi, C. (2019). Cap-specific, terminal N^6-methylation by a mammalian m^6Am methyltransferase. Cell Res. *29*, 80–82.

Sun, H., Li, K., Zhang, X., Liu, J., Zhang, M., Meng, H., and Yi, C. (2021). m^6Am-seq reveals the dynamic m^6Am methylation in the human transcriptome. Nat. Commun. *12*, 4778.

Tegowski, M., Flamand, M.N., and Meyer, K.D. (2022). scDART-seq reveals distinct m6A signatures and mRNA methylation heterogeneity in single cells. Mol. Cell *82*, 868–878.e10.

Thompson, M.G., Sacco, M.T., and Horner, S.M. (2021). How RNA modifications regulate the antiviral response. Immunol. Rev. *304*, 169–180.

van Tran, N., Ernst, F.G.M., Hawley, B.R., Zorbas, C., Ulryck, N., Hackert, P., Bohnsack, K.E., Bohnsack, M.T., Jaffrey, S.R., Graille, M., and Lafontaine, D.L.J. (2019). The human 18S rRNA m6A methyltransferase METTL5 is stabilized by TRMT112. Nucleic Acids Res. *47*, 7719–7733.

Wang, X., Lu, Z., Gomez, A., Hon, G.C., Yue, Y., Han, D., Fu, Y., Parisien, M., Dai, Q., Jia, G., et al. (2014). N6-methyladenosine-dependent regulation of messenger RNA stability. Nature *505*, 117–120.

Wang, Y., Zhao, Y., Bollas, A., Wang, Y., and Au, K.F. (2021). Nanopore sequencing technology, bioinformatics and applications. Nat. Biotechnol. *39*, 1348–1365.

Wang, X., Zhao, B.S., Roundtree, I.A., Lu, Z., Han, D., Ma, H., Weng, X., Chen, K., Shi, H., and He, C. (2015). N(6)-methyladenosine Modulates Messenger RNA Translation Efficiency. Cell *161*, 1388–1399.

Villanueva, L., Álvarez-Errico, D., and Esteller, M. (2020). The contribution of epigenetics to cancer immunotherapy. Trends Immunol. *41*, 676–691.

Wang, J., Alvin Chew, B.L., Lai, Y., Dong, H., Xu, L., Balamkundu, S., Cai, W.M., Cui, L., Liu, C.F., Fu, X.Y., et al. (2019). Quantifying the RNA cap epitranscriptome reveals novel caps in cellular and viral RNA. Nucleic Acids Res. *47*, e130.

Wang, Y., Xiao, Y., Dong, S., Yu, Q., and Jia, G. (2020). Antibody-free enzyme-assisted chemical approach for detection of N^6-methyladenosine. Nat. Chem. Biol. *16*, 896–903.

Weeks, K.M. (2021). SHAPE directed discovery of new functions in large RNAs. Acc. Chem. Res. *54*, 2502–2517.

Weng, X., Gong, J., Chen, Y., Wu, T., Wang, F., Yang, S., Yuan, Y., Luo, G., Chen, K., Hu, L., et al. (2020). Keth-seq for transcriptome-wide RNA structure mapping. Nat. Chem. Biol. *16*, 489–492.

Wetzel, C., and Limbach, P.A. (2016). Mass spectrometry of modified RNAs: recent developments. Analyst (Lond.) *141*, 16–23.

Yang, J., Sharma, S., Watzinger, P., Hartmann, J.D., Kötter, P., and Entian, K.D. (2016). Mapping of complete set of ribose and base modifications of yeast rRNA by RP-HPLC and mung bean nuclease assay. PLoS ONE *11*, e0168873.

Xiao, W., Adhikari, S., Dahal, U., Chen, Y.S., Hao, Y.J., Sun, B.F., Sun, H.Y., Li, A., Ping, X.L., Lai, W.Y., et al. (2016). Nuclear m6A reader YTHDC1 regulates mRNA splicing. Mol. Cell *61*, 507–519.

Yang, X., Liu, Q.L., Xu, W., Zhang, Y.C., Yang, Y., Ju, L.F., Chen, J., Chen, Y.S., Li, K., Ren, J., et al. (2019). m^6A promotes R-loop formation to facilitate transcription termination. Cell Res. *29*, 1035–1038.

Zaccara, S., Ries, R.J., and Jaffrey, S.R. (2019). Reading, writing and erasing mRNA methylation. Nat. Rev. Mol. Cell Biol. *20*, 608–624.

Zhang, L.S., Liu, C., Ma, H., Dai, Q., Sun, H.L., Luo, G., Zhang, Z., Zhang, L., Hu, L., Dong, X., and He, C. (2019). Transcriptome-wide mapping of internal N7-methylguanosine methylome in mammalian mRNA. Mol. Cell *74*, 1304–1316.e8.

Zhang, Z., Chen, T., Chen, H.X., Xie, Y.Y., Chen, L.Q., Zhao, Y.L., Liu, B.D., Jin, L., Zhang, W., Liu, C., et al. (2021). Systematic calibration of epitranscriptomic maps using a synthetic modification-free RNA library. Nat. Methods *18*, 1213–1222.

Zheng, Q., Hou, J., Zhou, Y., Li, Z., and Cao, X. (2017). The RNA helicase DDX46 inhibits innate immunity by entrapping m^6A-demethylated antiviral transcripts in the nucleus. Nat. Immunol. *18*, 1094–1103.

Zhou, H., Rauch, S., Dai, Q., Cui, X., Zhang, Z., Nachtergaele, S., Sepich, C., He, C., and Dickinson, B.C. (2019). Evolution of a reverse transcriptase to map N^1-methyladenosine in human messenger RNA. Nat. Methods *16*, 1281–1288.

Zhu, Y., Pirnie, S.P., and Carmichael, G.G. (2017). High-throughput and site-specific identification of *2′-O*-methylation sites using ribose oxidation sequencing (RibOxi-seq). RNA *23*, 1303–1314.

Zubradt, M., Gupta, P., Persad, S., Lambowitz, A.M., Weissman, J.S., and Rouskin, S. (2017). DMS-MaPseq for genome-wide or targeted RNA structure probing in vivo. Nat. Methods *14*, 75–82.